Available online at www.sciencedirect.com
ScienceDirect
Journal of the Mechanics and Physics of Solids
55 (2007) 1196–1211

JOURNAL OF THE MECHANICS AND PHYSICS OF SOLIDS

www.elsevier.com/locate/jmps

Spherical indentation of incompressible rubber-like materials

A.E. Giannakopoulos*, A. Triantafyllou

Laboratory for Strength of Materials and Micromechanics, Department of Civil Engineering, University of Thessaly, Volos 38336, Greece

Received 24 August 2006; received in revised form 31 October 2006; accepted 25 November 2006

Abstract

In recent years, indentation tests have been proven very useful in probing mechanical properties of small volumes of materials. However, a class of materials that very little has been done in this direction is rubber-like materials (elastomers). The present work investigates the spherical indentation of incompressible rubber-like materials. The analysis is performed in the context of second-order hyperelasticity and is accompanied by finite element computations and an extensive experimental program with spherical indentors of different radii. Uniaxial tensile tests were also performed and it was found that the initial elastic modulus correlates well with the indentation response. The experiments suggest stiffer indentation response than that predicted by linear elasticity, which is somehow counter-intuitive, if the uniaxial material response is to be considered. Regarding the uniqueness of the inverse problem, that is to establish material properties from spherical indentation tests, the answer is disappointing. We prove that the inverse problem does not give unique answer regarding the constitutive relation, except for the initial stiffness.

Keywords: Rubber materials; Incompressibility; Spherical indentation; Hyperelasticity; Inverse problems

1. Introduction

Elastomers are polymer materials with module of elasticity (typically) between 1 and 500 MPa and are characterized by large stains under stress. Of particular technological

*Corresponding author. Tel.: +30 2421 74179; fax: +30 2421 74169.
E-mail address: agiannak@uth.gr (A.E. Giannakopoulos).

0022-5096/$ - see front matter © 2006 Elsevier Ltd. All rights reserved.
doi:10.1016/j.jmps.2006.11.010

importance are rubbers that are manufactured from latex and may have a wide range of additives (carbon, silica, oils, kaolin, etc.). The elastic properties of these materials are achieved by cross-link of their molecules, for example by vulcanization with sulfur, at high temperatures (more than 150 °C) and under pressure. Applications of these materials include tires, springs, bearings, membranes, blades, hoses, conveyor belts, seals, pipes, etc. and are used extensively in cars, aircrafts, seals, buildings, bridges, railroads, cables and medical equipments. Important mechanical properties of rubber materials are that (a) they deform in a nearly incompressible manner (Poisson's ratio $n \to 0.5$) and (b) they are isotropic.

Currently, hardness testing of elastomers is based on the Shore test that uses the durometer (a hardened indenter with an accurately calibrated spring, a depth indicator and a flat presser foot). The Shore hardness is a number between 0 and 100, which has no obvious correlation with any fundamental mechanical property of the material (e.g. elastic modulus, uniaxial stress–strain response, etc.). Shore test methods are defined by various standards, e.g. ASTM D 2240, DIN 53505, etc. Elastomers have a Shore hardness number between 30 and 90. When strain rate effects are not important, the mechanical behavior of elastomers is modeled adequately by hyperelastisity, Green and Adkins (1970), Ogden (1984). In the context of hyperelastisity, the mechanical deformation of elastomers is captured by a variety of models which are accurate up to a certain level of straining, with the simplest models corresponding to low levels of straining. At this point, it is worth mentioning that hyperelastisity models serve well in the description of certain biomaterials, including the cells and the DNA. This is not very surprising, since the involved organic molecules are mainly long chains of covalently bonded carbon and hydrogen atoms, Treloar (1975).

Although hyperelasticity has been used extensively to obtain analytic and computational solutions to many problems (see for example, Antman (1995)), we have not encountered systematic contact analysis, other than the works of Choi and Shield (1981) and of Sabin and Kaloni (1983, 1989). Certain experimental work exists (see for example, Benabdallah and Chalifoux (1994)), however, little has been done to correlate experiments with hyperelastic contact analysis. In this work, we present some important results related to hyperelastic contact analysis, keeping in mind that the topic is very broad to be covered completely with the present paper. We have come across an important dilemma: what hyperelastic model should be used to extract a sufficiently general solution regarding the spherical indentation of a rubber substance by a rigid sphere of radius R? We concluded that a sufficiently general solution can be provided in the case of incompressibility and isotropy, but only if the indentation is not very deep, that is if the contact radius α is much smaller than the radius of the spherical indenter, $\alpha/R << 1$. This suggests a non-linear analysis of second order (moderate strains). Such analysis has been undertaken in the past by Choi and Shield (1981) and Sabin and Kaloni (1983). It is interesting to quote their results because both papers refer to the same material model and both provide second-order solutions to the spherical indentation problem, however, with different assumptions regarding the magnitudes of the strain invariants.

For incompressible rubber materials, Choi and Shield (1981) predict the depth of indentation D and the applied vertical load P to be

$$D = \frac{\alpha^2}{R}, \quad P = \frac{16\mu\alpha^3}{3R}, \tag{1}$$

where μ is the shear modulus at zero straining. It is obvious that these results suggest that linear elasticity holds true to second order, since Eq. (1) is identical to the classic predictions of linear elasticity (see for example Johnson (1985)). On the other hand, Sabin and Kaloni (1989) found a very different second-order solution for an incompressible rubber material:

$$D=\frac{\alpha^2}{R}\left[1-\frac{4\alpha}{3\pi R}(1-\ln 2)\right],\quad P=\frac{16}{3}\,\mu\,\frac{\alpha^3}{R}\left[1+\frac{9\alpha}{4\pi R}\right] \tag{2}$$

Eq. (2) predicts a stiffer response than that predicted by linear elasticity (essentially Eq. (1)).

To the best of our knowledge, no experimental or analytic verification has been given for any of these models so far. We decided that such an effort was worth taking. We also decided that it was necessary to perform theoretical analysis with different hyperelastic material models and to use finite element calculations to clarify some issues. The results of our experimental and analytic efforts are presented in this work. The paper is structured as follows. The first part gives the description of the problem and the theoretical framework of the analysis. A second-order analysis follows and provides closed form solutions that connect the indentation depth D, the contact radius α, the radius of the sphere R and the applied vertical load P. The first part concludes with some important finite element calculations. The second part starts with uniaxial tensile tests on a particular rubber material and continues with indentation tests of the same material by steel spherical indentors of different radii. The second part concludes with direct comparison of the different models. Finally, we discuss the findings and propose an inverse methodology to predict mechanical properties of rubber materials from spherical indentation tests.

2. Basic equations and the boundary conditions

The equations of equilibrium and the boundary conditions for an elastic body in the absence of body and inertia force, neglecting terms of higher degree than the second of the space derivative of the displacement u_i can be formulated according to Rivlin (1953).

In line with the previous investigations, we assume an elastic strain density energy function W in the reference configuration of the form suggested by Murnaghan (1951):

$$W=\alpha_1 J_2+\alpha_2 J_1^2+\alpha_3 J_1 J_2+\alpha_4 J_1^3+\alpha_5 J_3, \tag{3}$$

where $\alpha_1,\alpha_2,\alpha_3,\alpha_4,\alpha_5$ are constants and J_1,J_2,J_3 are invariants of the Lagrange strain tensor

$$\gamma_{ij}=\frac{1}{2}\left(\frac{\partial u_i}{\partial x_j}+\frac{\partial u_j}{\partial x_i}+\frac{\partial u_k}{\partial x_i}\frac{\partial u_k}{\partial x_j}\right),$$

where x_i ($i=1, 2, 3$) are the Cartesian coordinates of a material point in the undeformed configuration. When expressed in terms of principal stretches $\lambda_1,\lambda_2,\lambda_3$.

$$J_1=I_1-3,\quad J_2=I_2-2I_1+3,\quad J_3=I_3-I_2-1 \tag{4}$$

and

$$I_1=\lambda_1^2+\lambda_2^2+\lambda_3^2,\quad I_2=\lambda_1^2\lambda_2^2+\lambda_2^2\lambda_3^2+\lambda_1^2\lambda_3^2,\quad I_3=\lambda_1^2\lambda_2^2\lambda_3^2. \tag{5}$$

Note that the constants α_1 and α_2 are related with the Lame constants λ, μ of the linear elasticity at small deformations ($\lambda_i \to 1$):

$$\lambda = 4(\alpha_1 + 2\alpha_2), \quad \mu = -2\alpha_1. \tag{6}$$

If the material is incompressible, then α_2 and $\alpha_3 \to \infty$ in such a way that $\alpha_3 - 2\alpha_2$ is finite.

We now let the total displacement be

$$u_i = \upsilon_i + w_i, \tag{7}$$

where υ_i and w_i are the first- and the second-order displacements, respectively, and define the linear stresses of the incremental problem as

$$\begin{aligned} \tau_{ik} &= 2[-\alpha_1 e'_{ik} + 2(\alpha_1 + 2\alpha_2)\Delta'\delta_{ik}], \\ e'_{ik} &= \frac{\partial \upsilon_i}{\partial x_k} + \frac{\partial \upsilon_k}{\partial x_i}, \quad \Delta' = \frac{1}{2}\, e'_{ss} \end{aligned} \tag{8}$$

and

$$\begin{aligned} \tau''_{ik} &= 2[-\alpha_1 e''_{ik} + 2(\alpha_1 + 2\alpha_2)\,\Delta''\delta_{ik}], \\ e''_{ik} &= \frac{\partial w_i}{\partial x_k} + \frac{\partial w_k}{\partial x_i}, \quad \Delta'' = \frac{1}{2}\, e''_{ss}. \end{aligned} \tag{9}$$

Keeping terms up to second order in υ_i and first order in w_i, we obtain the equilibrium equations:

$$\frac{\partial \tau_{ik}}{\partial x_k} + \frac{\partial \tau''_{ik}}{\partial x_k} + \left(\Delta'\delta_{sk} - \frac{\partial \upsilon_s}{\partial x_k}\right)\frac{\partial \tau_{ik}}{\partial x_k} + \frac{\partial \tau'_{ik}}{\partial x_k} = 0, \tag{10}$$

with surface traction in the undeformed body to be

$$T_i = \left[\Delta'\delta_{sk} - \frac{\partial u_s}{\partial x_k}\right] l_s \tau_{ik} + l_k(\tau_{ik} + \tau'_{ik} + \tau''_{ik}) \tag{11}$$

and l_k the direction cosines of the unit normal vector to the undeformed surface of the body. Note that δ_{sk} is the Kronecker's delta and repeated indices imply summation from 1 to 3 in the usual way.

In Eqs. (10) and (11) the stress τ'_{ik} is given as

$$\begin{aligned} \tau'_{ik} = 2[&(4\alpha_2 - 2\alpha_3 + \alpha_1)\Delta' e'_{ik} - \alpha_1 \alpha'_{ik} - (\alpha_1 - \alpha_5)E'_{ik} \\ &+ \{(\alpha_1 + 2\alpha_2)\alpha' + (\alpha_1 + \alpha_3)E' + 2(6\alpha_4 + 2\alpha_3 - \alpha_1 - 2\alpha_2)\Delta'^2\}\delta_{ik}], \end{aligned} \tag{12}$$

where E'_{ik} is the cofactor of e'_{ik}, $\alpha'_{ik} = \frac{\partial u_i}{\partial x_s}\frac{\partial u_k}{\partial x_s}$, $E' = E'_{ss}$ and $\alpha' = \alpha'_{ss}$.

Eq. (10) is satisfied, if

$$\frac{\partial \tau_{ik}}{\partial x_k} = 0, \tag{13}$$

$$\frac{\partial \tau''_{ik}}{\partial x_k} + X'_i = 0, \tag{14}$$

where body type of forces appear in the form:

$$X'_i = \left(\Delta'\delta_{sk} - \frac{\partial v_s}{\partial x_k}\right)\frac{\partial \tau_{ik}}{\partial x_s} + \frac{\partial \tau'_{ik}}{\partial x_k}. \tag{15}$$

If we solve (13) subject to the boundary conditions:

$$T_i = l_k \tau_{ik} \tag{16}$$

and then solve (14) subject to the boundary conditions:

$$T'_i = l_k \tau''_{ik} = -\left[\Delta\delta_{sk} - \frac{\partial v_s}{\partial x_k}\right] l_s \tau_{ik} - l_k \tau'_{ik}, \tag{17}$$

then the initial problem would be considered solved up to the second order in the space derivatives of the displacement functions. The stresses (second Piola–Kirchhoff stresses) of such second-order elasticity problem are approximated by superposition:

$$t_{ik} = \tau_{ik} + \tau'_{ik} + \tau''_{ik}. \tag{18}$$

2.1. Contact problem of a rigid indentor

We consider the contact problem of a rigid indentor whose axis of symmetry is normal to the contact plane. We choose cylindrical polar coordinates (r, θ, z) such that the contact plane is $z = 0$ (Fig. 1). The boundary conditions at the surface of the material are:

$$u_z(r, o) = D - f(r), \quad 0 \leqslant r \leqslant \alpha, \quad t_{zz}(r, 0) = 0, \quad r > \alpha \text{ and } t_{rz}(r, 0) = 0, \quad r > 0. \tag{19}$$

Here, α is the radius of the contact perimeter of the projected contact area to the horizontal surface and D the depth of penetration of the tip of the indentor into the half space. With the tip positioned at the origin of the coordinate system, the surface of the rigid indentor has the form $z = -f(r)$ so that $f(0) = 0$. Following Choi and Shield (1981), we write D as

$$D = \varepsilon D_1 + \varepsilon^2 D_2, \tag{20}$$

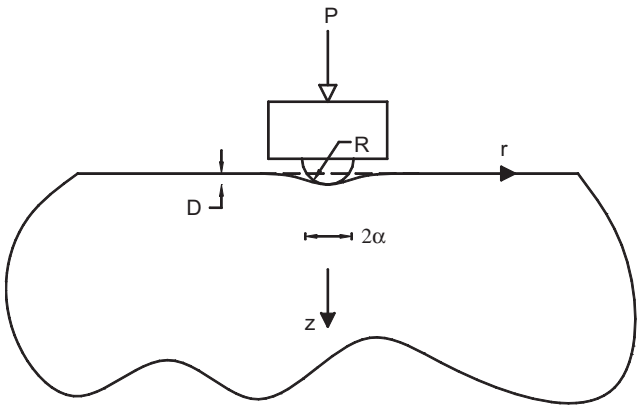

Fig. 1. Schematic of the spherical indentation problem.

where ε is a geometric parameter such that εD_1 represents the depth of penetration in the linear classical case. The term $\varepsilon^2 D_2$ represents the depth that would occur because of the consideration of the second-order displacements. From the previous section, we note that in order to solve this problem in second-order elasticity we must first solve Eq. (13) subject to the boundary conditions:

$$v_z(r,0) = \varepsilon D_1 - f(r), \quad 0 \leqslant r \leqslant \alpha, \quad \tau_{zz}(r,0) = 0, \quad r > \alpha, \quad \tau_{rz}(r,0) = 0, \quad r > \alpha. \tag{21}$$

The displacements and the stress fields for the linear problem are given by Johnson (1985) and Sneddon (1972). With the displacement components known, we can calculate the quantities $e'_{ij}, \Delta', \alpha'_{ik}, \alpha', E'_{ij}$ and E'. These strain-type quantities are used to obtain the expressions for τ_{ik} and τ'_{ik}, respectively, which are subsequently used in solving the second linear problem.

2.2. Solution of the second linear problem

The second linear problem to be solved is

$$\begin{aligned} &\frac{\partial \tau''_{rr}}{\partial r} + \frac{\partial \tau''_{rz}}{\partial z} + \frac{1}{r}(\tau''_{rr} - \tau''_{\theta\theta}) + X'_r = 0, \\ &\frac{\partial \tau''_{rz}}{\partial r} + \frac{\partial \tau''_{zz}}{\partial z} + \frac{1}{r}\tau''_{rr} + X'_z = 0, \end{aligned} \tag{22}$$

subject to the boundary conditions on the surface $z = 0$:

$$\begin{aligned} &\tau''_{rz}(r,0) = -T'_r \quad r \geqslant 0, \\ &w'_z(r,0) = \varepsilon^2 D_2 \quad 0 \leqslant r \leqslant \alpha, \\ &\tau'_{zz}(r,0) = -T'_z \quad r > \alpha \end{aligned} \tag{23}$$

and the conditions at infinity (zero displacements and stresses).

We make use of the linearity of the problem and consider the following three auxiliary problems, their superposition of which is equivalent to the initial problem (22) and (23)

$$\begin{aligned} &\tau''_{ik} = \sigma'_{ik} + \sigma''_{ik} + \sigma'''_{ik}, \\ &w_i = w'_i + w''_i + w'''_i. \end{aligned} \tag{24}$$

(i) Eqs. (22) subject to:

$$\begin{aligned} &\sigma'_{rz}(r,0) = 0 \qquad r \geqslant \alpha, \\ &w'_z(r,0) = 0 \qquad 0 \leqslant r \leqslant \alpha, \\ &\sigma'_{zz}(r,0) = -T'_z \quad r > 0. \end{aligned} \tag{25}$$

(ii) Eqs. (22) with $X'_r = X'_z = 0$, subject to:

$$\begin{aligned} &\sigma''_{rz}(r,0) = -T'_r \quad r \geqslant \alpha, \\ &w''_z(r,0) = 0 \qquad 0 \leqslant r \leqslant \alpha, \\ &\sigma''_{zz}(r,0) = 0 \qquad r > 0. \end{aligned} \tag{26}$$

(iii) Eqs. (22) with $X_r''=X_z''=0$, subject to:

$$\begin{aligned}&\sigma_{rz}'''(r,0)=0 && r\geqslant\alpha,\\ &w_z'''(r,0)=\varepsilon^2 D_2 && 0\leqslant r\leqslant\alpha,\\ &\sigma_{zz}'''(r,0)=0 && r>0.\end{aligned} \tag{27}$$

We can determine problems (i) and (ii) following Sabin and Kaloni (1983, 1989). Problem (iii), Eqs. (22) and (27), is simply equivalent to the problem of a flat circular punch on a linear elastic half space, Sneddon (1946). Superposing the results together, surface deformation is estimated from

$$u_z(r,0)=\upsilon_z(r,0)+w_z'(r,0)+w_z''(r,0)+w_z'''(r,0),\quad r>\alpha. \tag{28}$$

The distribution of pressure under the punch is given by

$$t_{zz}(r,0)=\tau_{zz}(r,0)+\tau_{zz}'(r,0)+\sigma_{zz}'(r,0)+\sigma_{zz}''(r,0)+\sigma_{zz}'''(r,0),\quad 0\leqslant r\leqslant\alpha \tag{29}$$

The total load P required to produce the penetration $D-f(r)$, $r<\alpha$ is given by

$$P=-2\pi\int_0^{\alpha} r t_{zz}(r,0)\mathrm{d}r. \tag{30}$$

2.3. Indentation by a spherical punch

We consider the case of the half space $z\geqslant 0$ deformed by the normal penetration of a rigid sphere of radius R, as shown in Fig. 1. For this problem, the spherical shape is approximated by

$$f(r)=\frac{r^2}{2R}. \tag{31}$$

If we take $\varepsilon=\alpha/R$ (with $\alpha/R<<1$), then

$$f(r)=\frac{\varepsilon r^2}{2\alpha}. \tag{32}$$

The orders of magnitude of the strain invariants in terms of $\varepsilon=\alpha/R$ are:

$$\begin{aligned}&J_1=0(\varepsilon), && J_2=0(\varepsilon^2), && J_3=0(\varepsilon^3),\\ &J_1^2=0(\varepsilon^2), && J_2J_1=0(\varepsilon^3), && J_1^3=0(\varepsilon^3).\end{aligned} \tag{33}$$

For compressible materials, the Poisson ratio n and the shear modulus μ at zero straining relate to the constants α_1 and α_2 as

$$\alpha_1=-\frac{\mu}{2},\quad \alpha_2=\frac{\mu(1-n)}{4(1-2n)}, \tag{34}$$

therefore, $n=(\alpha_1+2\alpha_2)/(\alpha_1+4\alpha_2)$.

To avoid the body forces in the equilibrium equations (neglecting terms of fourth and higher order in ε), we can take the constants α_3, α_4 and α_5 as

$$\alpha_3=\frac{\mu(5-6n)}{8(1-2n)},\quad \alpha_4=\frac{-3\mu(1-n)}{16(1-2n)},\quad \alpha_5=\frac{-3\mu}{4}. \tag{35}$$

In the incompressibility limit, the second-order solution depends only on α_1. Note that $n \to 0.5$, if $\alpha_2 \to \infty$ or if $\alpha_2 \to -\alpha_1/6$. Appendix A shows the uniaxial response predicted by a strain energy function of the form:

$$W = \alpha_1 J_2 - \frac{\alpha_1}{6} J_1^2 \tag{36}$$

($\alpha_1 = -1.3$ MPa for the material used in our experiments). This choice of W, although very satisfactory for the analysis of the indentation problem, gives stiffer response in uniaxial tension, as shown in Fig. A.1. We emphasize that (36) does not constitute actual material behavior, but is a fictitious response useful for the indentation analysis.

Following Sabin and Kaloni (1983, 1989), after some lengthy algebra, we obtain in the incompressible limit:

$$D_1 = \alpha, \tag{37}$$

$$D_2 = \frac{\alpha}{3\pi}(2 - 5 \ln 2) = -0.1555\alpha, \tag{38}$$

therefore,

$$D = \alpha\varepsilon(1 - 0.1555\varepsilon) = \frac{\alpha^2}{R}\left(1 - 0.1555\frac{\alpha}{R}\right) \tag{39}$$

and the total load is given as

$$P = \frac{16}{3}\alpha^2\varepsilon\mu\left(1 + \frac{9\varepsilon}{4\pi}\right). \tag{40}$$

The final relations (39) and (40) are presented in Fig. 2, together with the results (1) and (2). Note that Eq. (40) agrees with that of Sabin and Kaloni (1983), however, Eq. (39) does not. Even though the difference between (39) and (2a) seems to be small, it gives a noticeable difference in the P–D relation, since D is raised to the power 1.5. The present results, Eqs. (39) and (40) suggest a stiffer force–depth (P–D) relation compared to linear elasticity and to Sabin and Kaloni solution.

2.4. Spherical contact of a Mooney–Rivlin material

A more traditional strain energy density function for incompressible rubber (valid up to moderate levels of strain) is the Mooney–Rivlin type:

$$W = c_1 J_1 + c_2(J_2 + 2J_1). \tag{41}$$

In this case, $\mu = 2(c_1 + c_2)$ is the shear modulus at zero straining ($c_1 = 1.34$ MPa and $c_2 = 0.0342$ MPa for the material used in our experiments). To avoid body forces in the equilibrium equations, $c_1 = c_2$. Therefore $W = c_1 J_2 + 3c_1 J_1$ and the uniaxial response of this fictitious response is shown in Fig. A.1. This is essentially a suggestion implied by Choi and Shield (1981). We repeated the previous analysis and ended with the remarkable result that the second-order elasticity solution is exactly the same as the one predicted by the linear incompressible elasticity:

$$D = \frac{\alpha^2}{R}, \quad P = \frac{16\mu\alpha^3}{3R}. \tag{42}$$

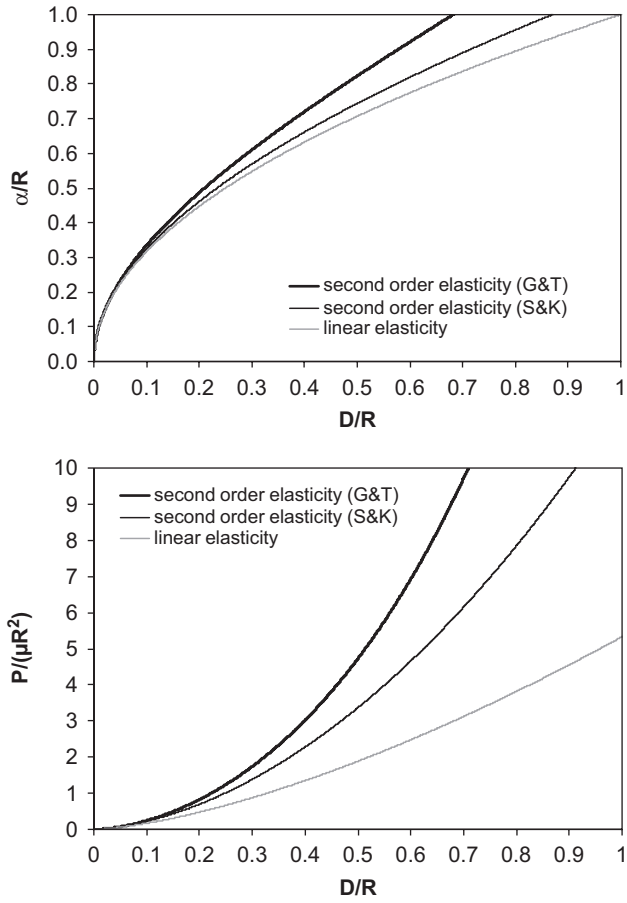

Fig. 2. Graphical representation of the present results (G&T) and comparison with the predictions of incompressible linear elasticity ($n = 0.5$) and with the predictions of Sabin and Kaloni (1983) (S&K).

To verify this important solution, we performed finite element calculations with ANSYS general-purpose finite element code, using the Mooney–Rivling material description with the following material constants: (a) $c_1 = c_2 = 0.6871$ MPa, (b) $c_1 = 1.3742$ MPa and $c_2 = 0$, (c) $c_1 = 1.34$ MPa and $c_2 = 0.0342$ MPa. A mesh of 5500 four-noded elements was used, arranged so that the near-the-contact area to be resolved by a regular 50×50 elements. The contact radius was resolved with at least 10–12 elements. The outer boundaries were away from the contact region by at least 20 times the maximum contact radius. The elements were of mixed type (stresses and displacements were interpolated in the virtual work scheme) to avoid locking and hourglass type of deformations due to material incompressibility. The contact was modeled without friction. The contact radii were $R = 0.75$ cm and 0.5 cm and the maximum indentation depth was $R/2$. Details of the finite element analysis are given elsewhere (Giannakopoulos and Panagiotopoulos, 2007). The finite element results confirmed and strengthened the result of Eq. (42), with $\mu = 2(c_1 + c_2)$ for all values of c_1 and c_2 that provide stable material response (and not only for

$c_1 = c_2$, as suggested by Choi and Shield). This, unfortunately, shows that the inverse problem of finding the functional form of W through indentation is not unique (only the sum $c_1 = c_2$ can be determined uniquely in this case).

3. Experiments

For the experimental part of this work, we used an incompressible rubber material with maximum tensile engineering stress of 18.37 MPa, at maximum tensile strain of 261.03% (according to the manufacturer IMAS A.G.). The manufacturer gave the Shore hardness to be 75 (scale A). We measured the density of the material to be 1.207 gr/cm^3. All experiments were performed at temperature of $20 \pm 5\,^{\circ}$C and relative humidity of 30%. We tested the material in uniaxial tension with a uniaxial tension/compression machine (MTS Q Test/1L Elite Controller), of maximum load ± 1 kN and accuracy of $\pm 10^{-2}$ N in force and $\pm 10^{-2}$ mm in displacements. The tests were performed with displacement control, according to the ASTM standards (D638, E8, D882, D3574 Part E, D412 A and B). A typical uniaxial tensile response is shown in Fig. 3 for a specimen with initial length $L_0 = 20.05$ mm and cross section $A_0 = 6.05 \times 1.89\,\text{mm}^2$. Fig. 3 shows the normalized force (engineering stress) F/A_0 versus the normalized elongation (strain) $\Delta L/L_0$. Also in Fig. 3 is the linearized initial response. The average initial elastic modulus was found to be $E_0 = 7.5 \pm 0.3$ MPa, corresponding to a shear modulus $\mu = E_0/3 = 2.5 \pm 0.1$ MPa. Loading speeds at 1, 5, 10 mm/min did not effect the material response. The data acquisition speed was 10 Hz.

For the indentation experiments, we modified the uniaxial machine by intervening a steel stage for the specimen that was fastened at the lower grip of the machine and a special mount for the spherical indentors that was fastened at the upper grip of the machine. We used spherical indentors of diameter $2R = 6.4$, 9.5, 12.7, 15 mm, all made from high strength steel St 360. The modulus of the indentor is 209 GPa, which is much higher than

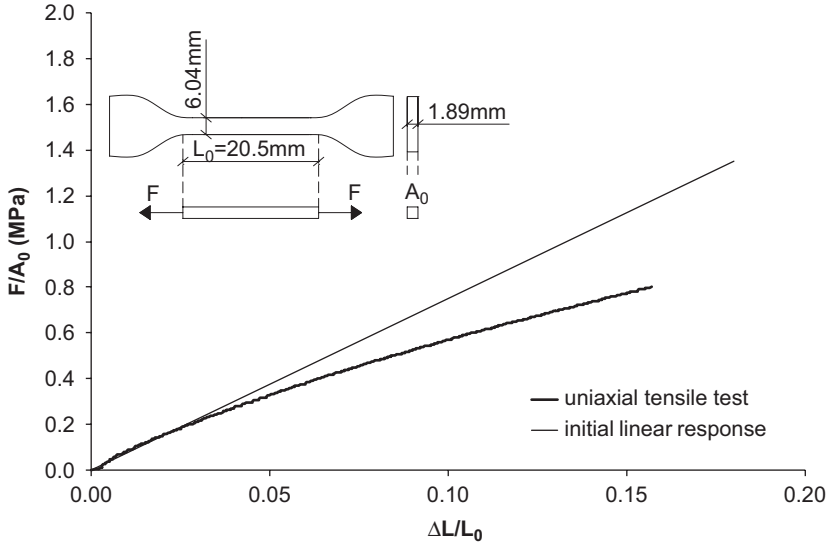

Fig. 3. Uniaxial tension experiment and the initial linear response ($E_0 = 7.5$ MPa).

that of the rubber material. The dimensions of the specimen ($135.3 \times 100 \times 30.5\,\mathrm{mm}^3$) were sufficiently large in all directions to avoid influence from the far field boundary conditions. The specimens were clamped on the stage. We used displacement control and the vertical velocity of the indentor was set to 1, 5, 10 mm/min, whereas the data acquisition speed was 10 Hz and in some cases 5 Hz. The indentation responses were not influenced by these parameters at all and showed remarkable repeatability and completely elastic behavior. Although it is well known that friction is not an issue for incompressible materials, certain experiments were performed using lubricant at the contact surface, without affecting the indentation response. A photograph of the device and the mounted specimen is given in Fig. 4. The maximum vertical load of the machine is 1 kN. The accuracy of the measured load is $\pm 10^{-2}$ N and the accuracy of the displacement is $\pm 10^{-2}$ mm. All the indentation experiments were performed for maximum indentation depth $D \leqslant 0.1R$, so that the present analysis be valid. Typical force–depth responses are summarized in Fig. 5. The analysis of the experimental results suggests that our present theory describes the P–D curves very well. As a typical example, Fig. 6 shows the experimental response for $2R = 9.5$ mm and the analytical predictions of linear elasticity theory, of Sabin and Kaloni theory and the present theory, in all theoretical curves, we

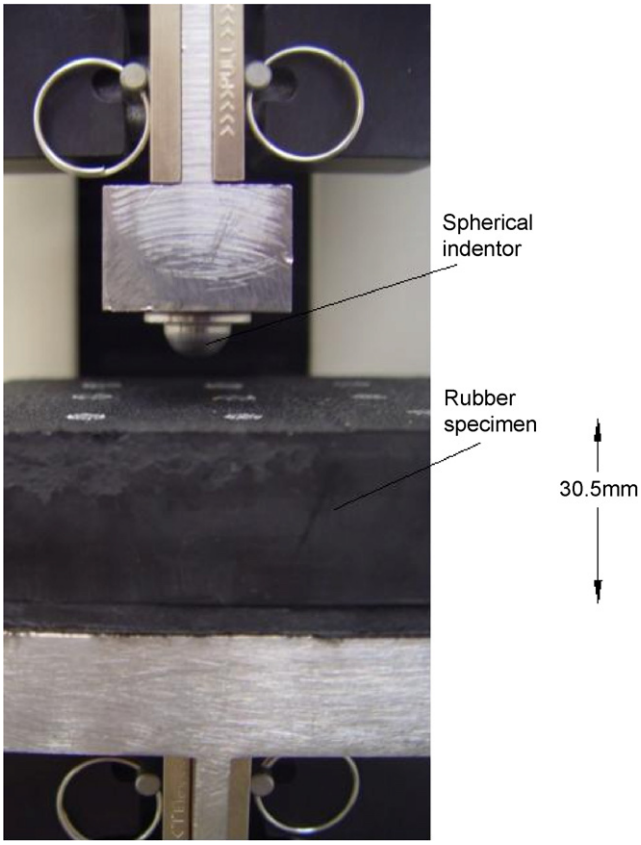

Fig. 4. Photograph showing the modified indentation machine with the rubber specimen mounted for testing.

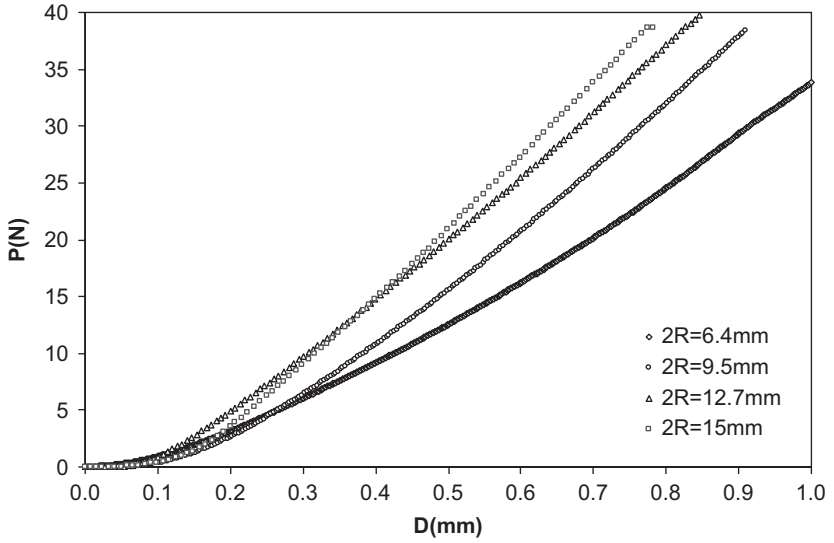

Fig. 5. Typical force–depth (P–D) experimental responses for different spherical indentors.

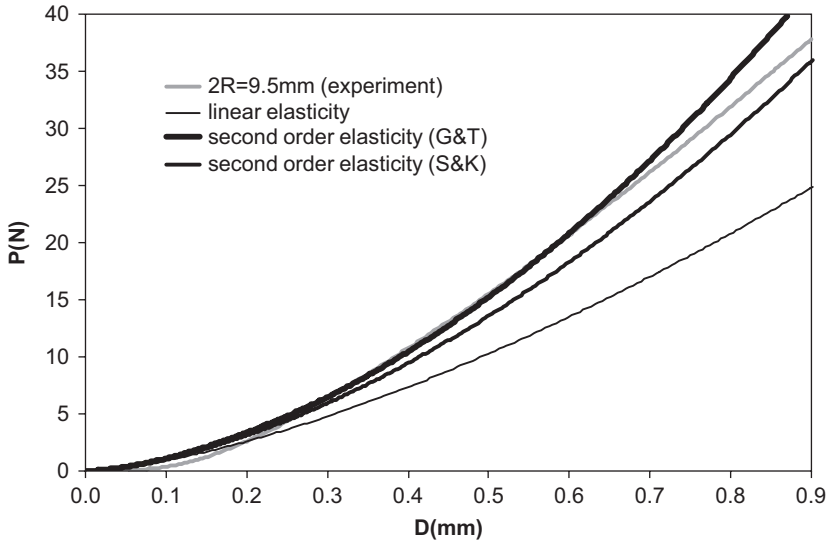

Fig. 6. Comparison of a typical experimental response ($R = 4.75$ mm) with the present work (G&T), with linear elasticity and with Sabin and Kaloni (1983) (S&K). All models use $\mu = 2.5$ MPa which corresponds to $E_0 = 7.5$ MPa.

used $\mu = 2.5$ MPa, as suggested by the uniaxial tensile experiments. The other experimental curves with different indentor's radii show similar trends.

In addition to the indentation experiments, we performed experiments to assess the imprint size α, for a spherical indenter $R = 5$ mm. The indenter was painted and subsequently loaded at three different loads $P = 48.1344,\ 98.1654,\ 148.4253$ N. Subsequently, the surfaces were examined upon unloading and the imprint radii were used

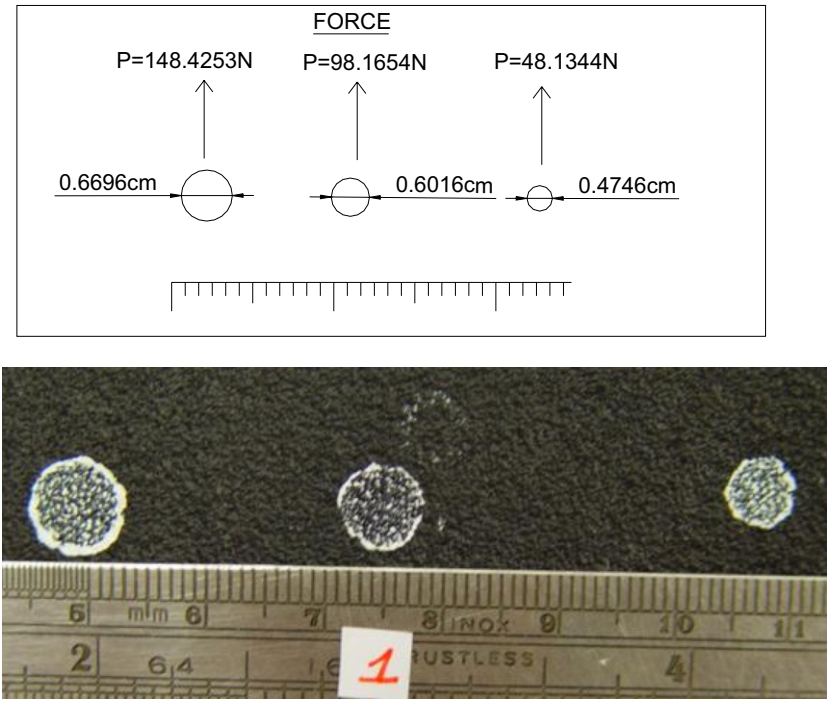

Fig. 7. Photograph of the contact imprints of a spherical indentor of radius $R = 5\,\text{mm}$ for three different load levels.

Table 1
The radii of the imprints for $R = 5\,\text{mm}$ and for different applied loads P, used for the inverse analysis of predicting the shear modulus μ by the various theoretical interpretations

Experimental data $R = 5\,\text{mm}$		Second-order elasticity (G&T)	Second-order elasticity (S&K)	Linear elasticity
P (N)	α (cm)	μ (MPa)	μ (MPa)	μ (MPa)
48.1344	0.2373	2.52	2.52	3.30
98.1654	0.2974	2.45	2.45	3.50
148.4253	0.3348	2.51	2.51	3.71

Uniaxial tensile test: $\mu = 2.5\,\text{MPa}$.

to obtain the elastic modulus of the material using the three different available theories. In this way, we performed an inverse analysis, checking at the same time the P–α relations. The results are very repeatable and some of them are shown in Fig. 7. We note that there is some uncertainty regarding the exact measure of the contact radius α, due to the paint accumulation of the contact perimeter. Since this paint accumulation is obvious from the photograph that does not belong to the contact area, we decided to exclude it from all measurements. Fitting the experimental results (P–α) in the analytic forms, we solved for the shear modulus μ and we reported it in Table 1. Note that our results agree with those of Sabin and Kaloni (1983), since both theories give the same P–α relation.

4. Conclusions

We have analyzed the indentation of incompressible rubber materials by rigid spheres and we found a new set of analytic expressions that relate the indentation depth D with the applied vertical force P, the contact radius α and the radius of the sphere R. The dominant material parameter is the shear modulus μ at zero straining. The analysis predicts that the indentation response is stiffer than that predicted by linear elasticity. Our relation between P and α is similar to that by Sabin and Kaloni (1983), however our P–D relation is stiffer than their results. Our analytic results are of second order and are valid for $D/R \leqslant 0.1$. An alternative material model, the well-known Mooney–Rivlin, gave results that are identical with the predictions of linear incompressible elasticity. This remarkable result is unfortunate for the reverse problem of estimating material properties from instrumented spherical indentation, because the two material constants involved in the Mooney–Rivlin model appear as a sum.

We have performed experiments on a typical incompressible rubber material used in conveyor belts. We investigated the response of this material in order to assess our analytic results, as well as other existing theoretical results. The experimental results support our analysis. Regarding the inverse problem, we conclude that it is possible to obtain the initial shear modulus (at zero straining) with reasonable accuracy. However, the exact form of the strain energy function cannot be captured by second-order analysis. The linear elasticity analysis underpredicts the shear modulus and this has to be considered in the investigation of rubber-like materials (including certain biomaterials) via indentation techniques. The results are of great value in the assessment of the true elastic properties of incompressible rubber materials and their correlation with fatigue strength.

Acknowledgements

The authors are grateful to the IMAS A. G. (Volos, Greece) company for providing the rubber material used in this investigation. We are also grateful to the Maranoglou et al. machine shop for manufacturing the indentors used in this work.

Appendix A. Uniaxial tensile response

At low strains, we approximate the strain energy function (3) by

$$W = \alpha_1 \left(J_2 - \frac{J_1^2}{6} \right), \tag{A.1}$$

where $\mu = -2\alpha_1$ is the shear modulus at zero straining.

In this case the strain invariants are:

$$J_1 = \lambda_1^2 + \lambda_2^2 + \lambda_3^2 - 3, \tag{A.2}$$

$$J_2 = \lambda_1^2\lambda_2^2 + \lambda_2^2\lambda_3^2 + \lambda_3^2\lambda_1^2 - 2(\lambda_1^2 + \lambda_2^2 + \lambda_3^2) + 3 \tag{A.3}$$

and the incompressibility condition is

$$\lambda_1\lambda_2\lambda_3 = 1, \tag{A.4}$$

where $\lambda_1, \lambda_2, \lambda_3$ are the principal stretches ($\lambda_1, \lambda_2, \lambda_3 > 0$).

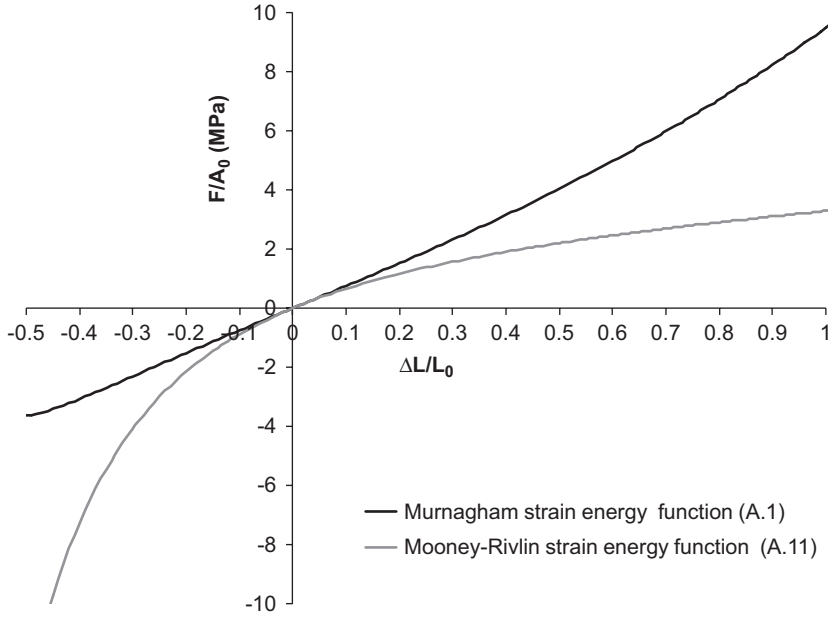

Fig. A.1. The uniaxial response for $W=\alpha_1 J_2-\alpha_1 J_1^2/6$ ($\alpha_1=-1.25\,\mathrm{MPa}$) and for $W=c_1 J_2+3c_1 J_1$ ($c_1=0.625\,\mathrm{MPa}$).

The principal Cauchy (true) stresses are:

$$\sigma_1=\frac{\partial W}{\partial \lambda_1}\lambda_1+p, \tag{A.5}$$

$$\sigma_2=\frac{\partial W}{\partial \lambda_2}\lambda_2+p, \tag{A.6}$$

$$\sigma_3=\frac{\partial W}{\partial \lambda_3}\lambda_3+p, \tag{A.7}$$

where p is a penalty stress due to incompressibility.

The boundary conditions for uniaxial tensile test of an orthogonal prism with initial area A_0 and initial length L_0 are:

$$\sigma_3=\sigma_2=0, \tag{A.8}$$

$$\sigma_1=\frac{F}{A}, \tag{A.9}$$

where F is the applied tensile force and A is the current cross section.

Isotropy suggests $\lambda_2=\lambda_3$. From (A.4) we have $\lambda_2^2=1/\lambda_1$ and therefore $A=A_0/\lambda_1$.

Note that λ_1 is related to the strain $\Delta L/L_0$ by $\lambda_1=1+\Delta L/L_0$ (ΔL is the change of length). Using the boundary condition (A.8), we can define p and then

$$\sigma_1=\mu\left[\frac{1}{3}\lambda_1^4+\lambda_1^2-\frac{2}{3}\lambda_1+\frac{1}{3}\frac{1}{\lambda_1^2}-\frac{1}{\lambda_1}\right]=\frac{F}{A_0}\lambda_1. \tag{A.10}$$

For the approximate Mooney–Rivlin strain energy function:

$$W = c_1 J_2 + 3c_1 J_1, \tag{A.11}$$

where $\mu = 4c_1$ is the shear modulus at zero straining and by using the same analysis as shown above, we find

$$\sigma_1 = \frac{\mu}{2}\left[\lambda_1^2 + \lambda_1 - \frac{1}{\lambda_1^2} - \frac{1}{\lambda_1}\right] = \frac{F}{A_0}\,\lambda_1. \tag{A.12}$$

Eqs. (A.10) and (A.12) are plotted in Fig. A.1 for $\alpha_1 = -1.25\,\text{MPa}$ and $c_1 = 0.625\,\text{MPa}$, that is in both cases $E_0 = 7.5\,\text{MPa}$.

References

Antman, S.S., 1995. Nonlinear Problems of Elasticity. Springer, New York.

Benabdallah, H., Chalifoux, J.P., 1994. Small depth indentation of plastic materials. Polym. Test. 13, 377–397.

Choi, I., Shield, R.T., 1981. Second order effects in problems for a class of elastic materials. J. Appl. Math. Phys. (ZAMP) 32, 361–381.

Giannakopoulos, A.E., Panagiotopoulos, D., 2007. Hyperelastic contact analysis by finite elements, in preparation.

Green, A.E., Adkins, J.E., 1970. Large Elastic Deformations, second ed. Charendon Press, Oxford.

Johnson, K.L., 1985. Contact Mechanics. Cambridge University Press, Cambridge.

Murnaghan, F.D., 1951. Finite Deformations of an Elastic Solid. Wiley, New York.

Ogden, R.W., 1984. Non-Linear Elastic Deformations, Eds. Harwood Series Mathematics and its Applications.

Rivlin, R.S., 1953. The solutions of the problems in second order elasticity theory. J. Ration. Mech. Anal. 2, 53–81.

Sabin, G.C.W., Kaloni, P.N., 1983. Contact problem of a rigid indentor in second order elasticity theory. J. Appl. Math. Phys. 34, 370–386.

Sabin, G.C.W., Kaloni, P.N., 1989. Contact problem of a rigid indentor with notational friction in second order elasticity. Int. J. Eng. Sci. 27, 203–217.

Sneddon, I.N., 1946. Boussinesq's problem for a flat-ended cylinder. Proc. Cambridge Phil. Soc. 42, 29–39.

Sneddon, I.N., 1972. The Use of Integral Transforms. Mc Graw-Hill, New York.

Treloar, L.R.G., 1975. The Physics of Rubber Elasticity, third ed. Clarendon Press, Oxford.